

# PROPAGATING PARTICLES THROUGH INHOMOGENEOUS SCALAR FIELDS

Gerd Reis and Martin Bertram  
Intelligent Visualization and Simulation  
DFKI GmbH Kaiserslautern  
Germany  
email: {reis, herbert}@dfki.uni-kl.de

## ABSTRACT

We present a numerical integration scheme for the propagation of particles/rays within continuous, inhomogeneous media, represented as discrete scalar fields. Our method aims at the calculation of energy distribution, where the initial energy is evenly distributed over a large number of particles, which are traced through the medium. While traversing the particles interact with the medium by means of absorption, reflection and refraction. To calculate these paths, we construct a numerical integration formula based on refraction and reflection laws given for rigid material boundaries. Numerical examples show that our method correctly traces particles/rays within e.g. curved optical fibers with a circular cross-section density.

## KEY WORDS

particle tracing, ultrasound, simulation, refraction

## 1 Introduction

Particle tracing is often used to model the propagation of optical and acoustic waves. Prominent examples are bi-directional ray-tracing methods like photon tracing [1] and equivalent methods in geometric acoustics [2, 3]. Unfortunately, most approaches are based on linear ray-tracing and do not consider the influence of completely inhomogeneous media on the ray/particle direction. The only case where reflection and refraction rules are correctly applied is at rigid material interfaces.

Especially in the field of medical visualization the underlying data sets are given as discrete scalar/vector data on a regular grid. This data most often contains features which are very small in extend and large in number, such that an effective modelling with boundary representations is not feasible. The same holds for smoothly varying regions. This in turn hinders simulation methods in approximating trajectories with e.g. poly-lines.

In order to simulate ultrasound images (see [4]) it is necessary to know the sound propagation paths, since these strongly affect the image generation process. This is especially apparent for ultrasound artifacts known as reverberation and mirroring. With existing methods this type of artifacts cannot be generated, since multiple reflections are not handled. The use of particle systems with general path tra-

jectories can handle these multiple reflections/refractions such that most kinds of artifacts can be generated.

In this work, we make the following contributions: We present a numerical integration scheme for tracing particle paths representing energy portions traversing a medium. The resulting trajectories are timeless, since for particles (in contrast to wave propagation) the interaction with the matter is independent from propagation speed. Applying the material dependant propagation speeds to the trajectories it is even possible to model runtime/depth artifacts for ultrasound images.

Although developed with special interest in simulating medical ultrasound images, our method facilitates a variety of applications such as acoustic simulations as well as photo-realistic rendering. Numerical examples suggest that our method provides correct results for different settings.

## 2 Related Work

This work is strongly related to techniques like non-linear ray-tracing [5] and particle tracing [6, 7]. These methods are similar, in that the ray/particle paths are influenced by the given setting, e.g. by gravitational forces, or refractions at object interfaces [8]. The main difference is that our method does not assume a quasi-homogenous setting, but handles a completely inhomogeneous medium with anisotropic effects. So the ray/particle-paths are not only affected at object boundaries (which is the case for e.g. glass objects). Despite that it is not possible to approximate geodesics by e.g. poly-lines, since the medium does not vary smoothly as is the case for e.g. a gravitational field.

Another similarity is given to wave propagation methods [9]. These methods can handle completely inhomogeneous media and the resulting energy distributions can be calculated. Other techniques that need to be mentioned in this regard are the *finite element methods*, which can be applied successfully to wave and particle propagation problems. Unfortunately these methods are computationally very expensive and expose unwanted and disturbing boundary effects (no method is known to handle perfectly absorbing boundaries).

Although the computational complexity can be reduced dramatically e.g. in using *Monte Carlo* based tech-

niques [10, 11] these methods can only be applied when special assumptions are valid for the underlying model. As an example assume dense random media. For the application in scope, i.e. simulation of ultrasound images such a model cannot be used since the human anatomy does expose significant structure.

As a last similarity the direct volume rendering needs to be mentioned. Neglecting sophisticated methods during the rendering process all the information needed to calculate non-uniform ray traversal is also generated to perform the color computation (e.g. gradients). The main difference of course is that the rays used for volume rendering are linear structures in general.

### 3 Implementation

There exist three fundamental cases how a particle is affected when traversing the scalar density field. First, the medium might be homogeneous. In this case the particle direction is not affected at all and the particle position can be calculated by moving an integral step into the given direction. The two other cases occur when the tissue density is not homogenous. In this case the particle travels from a region of lower density to a region with higher density or vice versa. Consider the two cases shown in figure 1. The law of refraction, also known as *Snell's law*, is given by

$$\frac{\sin \alpha_i}{\sin \alpha_t} = \frac{d_{thick}}{d_{thin}}, \quad (1)$$

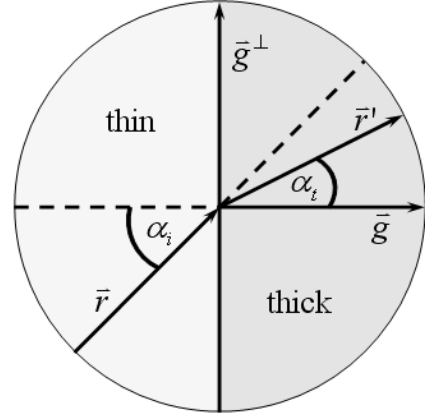
where  $d_*$  denote the respective densities,  $\alpha_i$  denotes the incidence angle and  $\alpha_t$  the transmit angle between the interface normal and the particle propagation direction. The law of reflection is given by

$$\angle(\vec{r}, \vec{n}) = \angle(\vec{r}', \vec{n}), \quad (2)$$

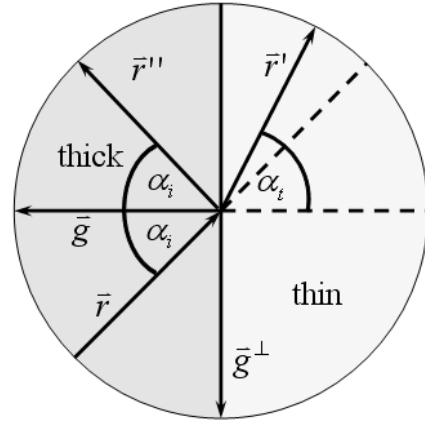
where  $\vec{r}$  is the particle propagation direction,  $\vec{r}'$  is the new particle direction and  $\vec{n}$  is the interface normal at the point of intersection. The vectors  $\vec{r}$ ,  $\vec{r}'$  and  $\vec{n}$  are assumed to be coplanar, which is always true for the two-dimensional case.

Looking at figure 1 it is obvious that two different density values are needed to calculate the the new direction. In the case of a density field (given as a discrete scalar map), one needs to adapt these refraction and reflection rules such that they can be applied to integrate rays (considered as particle trajectories) through a medium with varying density. Depending on the integral step size this point is not obvious for a discrete density field. To avoid expensive calculations we decided to formulate the density based on the discrete gradient information. For a position  $(x, y)$ , we define a density  $d_0$  at position  $(x, y)$  and the gradient vector

$$\vec{g}(x, y) = (d_{(x+1,y)} - d_{(x-1,y)}, d_{(x,y+1)} - d_{(x,y-1)}), \quad (3)$$



(a) refraction only



(b) refraction and total reflection

Figure 1. Different effects depending on the tissue density gradient

where  $d_{(x,y)}$  denotes the density value at position  $(x, y)$ . For a particle traversing in direction  $\vec{r}$  we calculate the tissue density beyond the interface according to

$$d_1 = d_0 + s \cdot \frac{\langle \vec{g} | \vec{r} \rangle}{\|\vec{g}\| \cdot \|\vec{r}\|} \cdot \vec{g}, \quad (4)$$

where  $\langle \cdot | \cdot \rangle$  is the Euclidean scalar product and  $s$  is the integration step. Since sub-pixel accurate calculations should be performed, the particle locations do not coincide with the pixel positions in general. Hence a bilinear interpolation is performed for the density value, the gradient direction as well as the gradient magnitude. The gradient is interpolated from precalculated values at the discrete map locations to gain computational speed.

Now, the pure refraction is investigated (see figure 1a). In order to calculate the refracted direction vector the

sines of the respective angles between the ray/particle direction  $\vec{r}$  and gradient are required. These are calculated by taking the inner product between the particle direction and a vector orthogonal to the gradient,

$$\vec{g}^\perp = (-g_y, g_x) \quad (5)$$

In total the sine of the angle between the refracted particle direction and the gradient is

$$\sin \alpha_t = \sin \alpha_i \cdot \frac{d_0}{d_0 + s \cdot \frac{\langle \vec{g} | \vec{r} \rangle}{\|\vec{g}\| \cdot \|\vec{r}\|} \cdot \vec{g}}, \quad (6)$$

where  $\alpha_i$  denotes the incident angle and  $\alpha_t$  the transmitted i.e. refracted angle. The respective cosine value can be calculated by using the equality

$$\sin^2 \alpha + \cos^2 \alpha = 1. \quad (7)$$

Having all necessary information at hand the refracted direction is calculated by rotating the direction vector towards the gradient. This is formulated as

$$\begin{aligned} \vec{r}'_x &= \vec{r}_x \cdot \cos \alpha_t - \vec{r}_y \cdot \sin \alpha_t \\ \vec{r}'_y &= \vec{r}_x \cdot \sin \alpha_t + \vec{r}_y \cdot \cos \alpha_t. \end{aligned} \quad (8)$$

The second case, i.e. when traversing from a higher density to a smaller one, is a bit more involved as depicted in figure 1 b). In principle the refraction is calculated as in the former case, bearing in mind that the gradient direction is inverted. However, the value for  $\sin \alpha_t$  can become greater than one when using equation 4. In this case the particle direction is not refracted any more, but reflected at the tissue boundary. This effect is known as *total reflection*. The reflected vector is calculated as follows

$$\vec{r}'' = \vec{r} - 2 \langle \vec{r} | \vec{g} \rangle \vec{g}. \quad (9)$$

Figure 2 gives a very simple example of the different effects. The particles are inserted into the medium with fan shaped directions at the left side. The intensity of the background indicates different densities of the medium. Lighter regions are denser than darker regions. The first interactions the particle undergoes are with homogeneous medium, so the path is not affected at all. Looking at the first interface one observes that the particle path is refracted towards the interface normal (gradient). At the second boundary the inner particles are transmitted and thereby refracted away from the interface normal, whereas the outer particles are reflected by the law of total reflection. The reflected particles again interact with the first interface, and again they are refracted away from the gradient direction.

Until now we investigated only the case of total reflection. Despite this effect reflection always occurs at a certain degree, depending on the properties of the participating media. For real world physical processes (e.g. acoustics, light

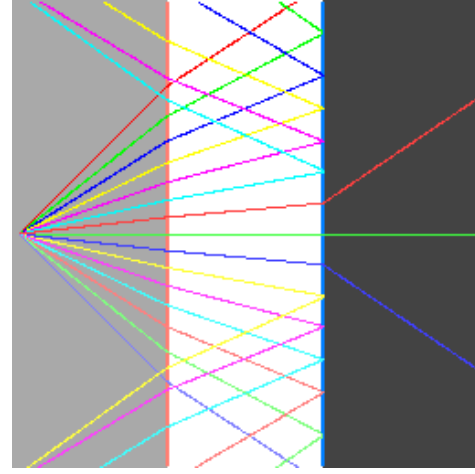


Figure 2. Refraction and reflection shown for a very simple configuration

transport, etc.) the tradeoff between reflection and refraction can be described as

$$\begin{aligned} R &= \frac{(Z_2 / \cos \alpha_t) - (Z_1 / \cos \alpha_i)}{(Z_2 / \cos \alpha_t) + (Z_1 / \cos \alpha_i)} \\ T &= \frac{2(Z_1 / \cos \alpha_i)}{(Z_2 / \cos \alpha_t) + (Z_1 / \cos \alpha_i)}, \end{aligned} \quad (10)$$

where  $\alpha_i$  is the incident angle and  $\alpha_t$  is the transmitted angle, which are related to each other by Snell's law (1).

Unfortunately a particle can undergo a single interaction only and can not be split (as would be the case for the energy distribution of light waves). Therefore this behavior needs to be modelled statistically. This is done in taking an evenly distributed random variable deciding whether a particle is reflected or transmitted. Then the raw energy of a particle is modulated according to equations 10.

As described above the particle/ray propagation method results in quite nice propagation paths for very simple settings as shown in figures 2 and 4. Applying the method to more general settings the expected effects are largely affected by the geometry, such that some kind of "geometric artifacts" will occur, which significantly disturb the final particle distribution. These artifacts develop due to the fact, that the particles have very distinct paths and travel within a discretized medium, such that particle groups are reflected in a very similar way resulting in sharp corners. This effect cannot be found in e.g. medical imaging and is in consequence disturbing. Ray-tracing obviously suffers from very similar problems due to pure specular reflections. However, in ray-tracing an appropriate local lighting model is used, to remedy the situation, for example the "Phong shading"-model. This model can be reformulated for the particle propagation process, to model diffusely reflecting boundaries. Therefore a distribution function is evaluated, which slightly alters the path of the reflected particles, adjusting the transmitted energy accordingly. This is depicted in figure 3. Since a concept-like "viewer" is not

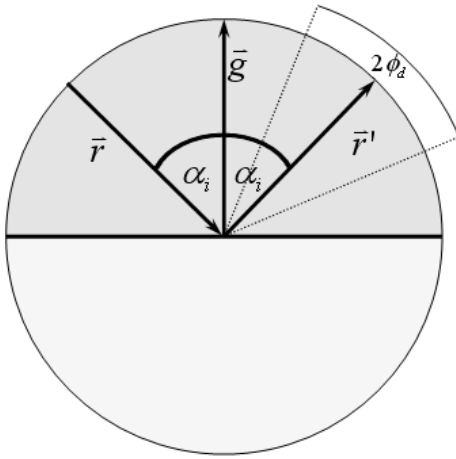


Figure 3. Distributing reflected rays

available, when tracing particles the angle between viewer and reflected ray - as used with the Phong model - needs to be given a priori. The valid angular range is given as  $[0, \pi/2]$ . Upon selecting an appropriate angle  $\phi_d$  the distribution weight is calculated according to

$$w(\phi_d, c) = \cos^c(\phi_d). \quad (11)$$

The parameter  $c$  is used in analogy to the material parameter of the Phong model. There are two plausible ways to interpret this parameter

- $c$  is associated to the density of the reflecting material, i.e.  $d_1$  in equation 4
- $c$  is associated to the density gradient magnitude of the respective interface, i.e.  $d_1/d_0$ .

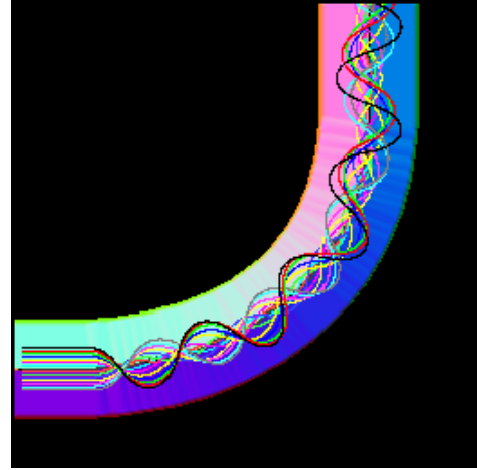
The first interpretation is based on the observation that the particle is reflected upon the material beyond the interface (as is done with normal ray-tracing), and the second interpretation is based on the observation, that the material in front of the interface significantly affects the reflection. The latter interpretation differs from ordinary ray-tracing, since ray-tracing does not assume any matter between objects. There are also several ways to interpret the weighting function  $w(\phi_d, c)$  itself e.g.

- $w$  is associated with a probability, distributing the resulting particle/ray direction while keeping the energy of a particle constant
- the particle directions are distributed evenly over the whole opening angle  $\phi_d$ , with  $w$  describing the according energy modulation.

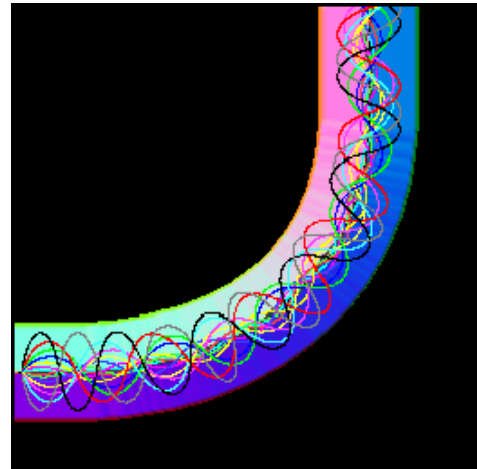
The former interpretation is useful, when a lossless scattering is assumed, i.e. no energy is lost in the scattering process (this could be assumed for light transport). The latter interpretation is used to model lossy scattering processes, where acoustic energy is transformed into heat energy, which is not available in the visualization process any longer (e.g. ultrasound).

## 4 Results

Figure 4 depicts particle trajectories in a particle guide (in analogy to wave guide), which can be identified with a light-wave cable. In subfigure a) the particles were injected in parallel, whereas in the subfigure b) the particles were injected fan shaped. The fact that both traces remain completely within the fiber and that the width of the trajectory track of the particle set does not increase with path length suggests that our integration method is physically correct and sufficiently accurate.



(a) The particles are injected in parallel at the lower left end

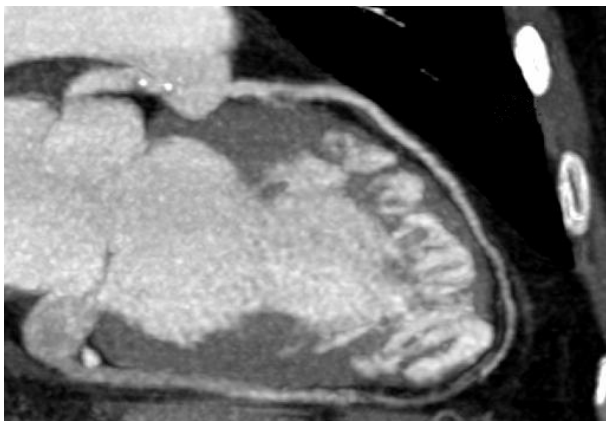


(b) The particles were injected fan shaped

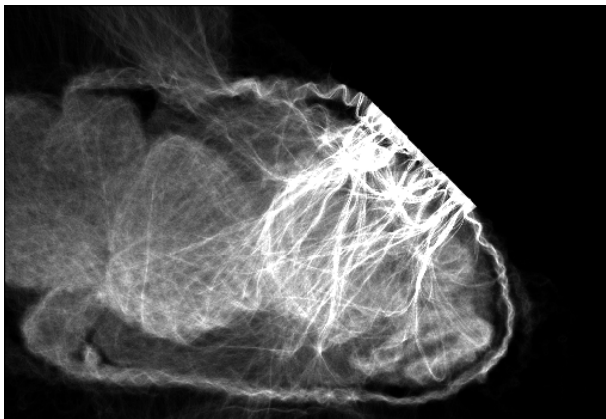
Figure 4. Particle guide (e.g. bent light-wave cable). The particles travel along the fibre and never leave it. Especially the diameter of the complete particle track remains constant.

Figure 5 gives a more practical example of the particle tracing. Subfigure a) depicts an inhomogeneous medium.

Please note that the material properties were selected by a transfer function, which firstly does not model real tissue parameters (as would be used for medical applications) and secondly was selected such that the resulting effects are clearly visible. The particles were injected in parallel from the upper right. The direction was chosen to be equal for all particles and points to the lower left. Interestingly, we do not get a homogenous distribution as shown in sub-figure b). Instead bunches of particles follow local features in the data set. Another really interesting point is, that the particles form energy accumulations at the lower feature interfaces, which is (at least in the context of ultrasound imaging) known as sedimentation.



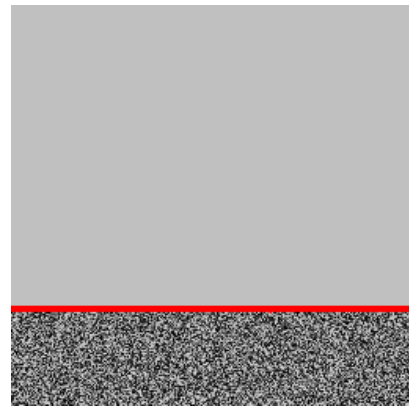
(a) The underlying tissue data which stems from an MRI data set and was transformed using an appropriate transfer function



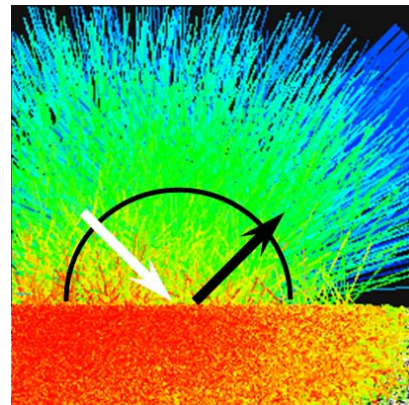
(b) The resulting intensity profile

Figure 5. The resulting intensity profile generated with particle tracing. Note the sedimentation at the feature bottom interfaces

A particle beam interaction with a reflector is depicted in figure 6. Subfigure (a) shows the definition of the reflector, subfigure (b) shows the resulting (truncated) particle traces and subfigure (c) a respective intensity profile.



(a) The reflector modelled as a homogenous interface upon inhomogeneous matter



(b) The resulting color coded particle trace (traces truncated for visibility)



(c) The intensity profile shows the diffuse reflection as well as the specular reflection at the right

Figure 6. Simulating a particle beam interaction for a complex reflector. Specular and diffuse reflection as well as sub-surface scattering occur

The particles were injected parallel to the white arrow. The main (specular) reflection direction is indicated by a black arrow. The colors of the particle trace were chosen as a transition from blue (high intensity) to red (low intensity). Please note, that the specular reflection is of high intensity, whereas the diffuse reflection is of significantly lower intensity. This can also be observed in the intensity profile, which was extracted over a semicircle centered at the

middle of the incident beam and at height of the reflector interface.

The particle beam first hits a homogeneous interface (marked in red figure 6(a)) at an angle of  $45^\circ$ . A subset of particles is directly reflected at the interface and produces the specular reflection which can be found at the right side of the image and in the intensity profile (figure 6(c)) respectively. The other particles traverse the interface and interact with the inhomogeneous medium, where they are scattered several times. Note that the traces of the scattered particles clearly show, that some will never leave the medium, whereas other particles will leave the medium at a significant distance from the incident beam.

## 5 Conclusion

We presented a new integration scheme for the propagation of particles in inhomogeneous data fields. This type of propagation is suited to model energy propagation for e.g. ultrasound image simulation. Using the proposed method very important types of artifacts, namely reverberation and mirroring can be investigated which is not possible with existing methods. Although called artifacts (with respect to visualization) these phenomena are an integral and important component of ultrasound images and need to be modelled appropriately to get realistic looking results.

Despite the application of ultrasound image simulation the propagation scheme can be used to implement inhomogeneous materials in ray/photon-tracing as well in phonon-tracing. The method can be easily extended to higher dimensions and can also incorporate vector valued data instead of the scalar data, such that frequency dependant behavior can be introduced.

## References

- [1] H.W. Jensen and P.H. Christensen. Efficient simulation of light transport in scene with participating media using photon maps. In *Computer Graphics (SIGGRAPH 98)*, pages 311–320, July 1998.
- [2] T. Funkhouser, I. Carlbom, G. Elko, G. Pingali, M. Sondhi, and J. West. A beam tracing approach to acoustic modeling for interactive virtual environments. In *Computer Graphics (SIGGRAPH 98)*, pages 21–32, Orlando, FL, July 1998.
- [3] J. Mohring J. Jegorovs M. Bertram, E. Deines and H. Hagen. Phonon tracing for auralization and visualization of sound. In *Proceedings of IEEE Visualization 2005*, pages 151–158, 2005.
- [4] K. Schwenk, G. Reis, and R.H. van Lengen. Real-time artificial ultrasound images. In *Submitted to 2005/06 Elsevier Journal Simulation Modelling Practice and Theory*, 2005.
- [5] Daniel Weiskopf. Four-dimensional non-linear ray tracing as a visualization tool for gravitational physics. pages 445–448, 2000.
- [6] I.M. Razso. Particle tracing methods in photorealistic image synthesis, 1998. <http://www.cg.tuwien.ac.at/studentwork/CESC/G98/IMRazso/index.html>.
- [7] Z. Hakura and J. Snyder. Realistic reflections and refractions on graphics hardware with hybrid rendering and layered environment maps. In *In Proceedings of the 12th Eurographics Workshop on Rendering*, 2001.
- [8] M.A. Shah, J. Kontinen, and S. Pattanaik. Caustics mapping: An image-space technique for real-time caustics. In *To appear in IEEE Transactions on Visualization and Computer Graphics (TVCG)*, 2006.
- [9] A. Garriga, C. Spa, and V. Lpez. Computation of the complete acoustic field with finite-differences algorithms, 2005. Forum Acousticum 2005, Budapest.
- [10] S. A. Prahl, M. Keijzer, S. L. Jacques, and A. J. Welch. A monte carlo model of light propagation in tissue. In *In SPIE Proceedings of Dosimetry of Laser Radiation in Medicine and Biology*, volume IS 5, pages 102–111, 1989.
- [11] B. E. Barrowes, C. O. Ao, F. L. Teixeira, J. A. Kong, , and L. Tsang. Monte carlo simulation of electromagnetic wave propagation in dense random media with dielectric spheroids. In *IEICE Trans. Electronics*, volume E83-C, page 1797, Dec. 2000.